

We thank the Referee for the very insightful comments. We have revised our manuscript according to the suggestions of the Referee's comments and our responses to the comments are as follows. Referee's comments are in black, authors' responses are in blue, and changes to the manuscript are in red color text.

In this work, the authors studied the photooxidation of furan and the resulting secondary organic aerosol formation. In particular they investigated the effect of NO_x level and relative humidity on the yields and chemical composition of SOA. The experiments were conducted with a laboratory chamber and measurements by SMPS, FTIR, and ESI-MS formed the basis for the main experimental results. The topic is of interest to ACP's audience and fits within the scope of ACP. However, the results are too general and inconclusive and there are a few issues with experimental design. I do not recommend publication in ACP at this point.

1. First of all, it is unclear what the insights are from the presented set of results. The manuscript presents trends in yields with NO_x/humidity, but there is no experimental investigation that would elucidate the "why". For example, the increase in yields with increasing NO_x is consistent with isoprene photooxidation studied by Kroll et al. (2006). That is true only for high VOC/NO_x ratio. In all other studies, NO tends to suppress yields. So why for furan at these VOC/NO_x ratios, the trend is positive with NO_x? What is special about furan? What is NO, or NO₂, or NO_x doing that would change the volatility of the products? A similar set of questions would also be raised regarding RH. What are the reactions that are affected by water, and would affect yields? The measurements of composition and yields are not sufficiently tied together to present a holistic story. Without these mechanistic insights, it is hard to generalize the findings and NO_x/RH effects to make this an impactful study. The lack of any proposed or cited mechanisms in the main body of the manuscript make the results seem like an isolated set of findings and therefore do not advance the knowledge of SOA formation.

Author reply:

In generally, NO_x can have two different effects on SOA formation. Increasing NO_x concentration will promote the formation of O₃ and HONO, leading to more OH radical formed, which in turn is favorable to SOA formation (Sarrafzadeh et al., 2016). In addition, high NO_x level can facilitate the competition between NO/NO₂ and HO₂ to react with RO₂. Products with high volatility will be generated more by the NO_x+RO₂ reaction than the HO₂+RO₂ reaction (Kroll and Seinfeld, 2008). However, the formation of lower volatility products is favored by the increase of SOA yields (Chen et al., 2018). In this regard, the increasing NO_x level is not conducive to SOA formation. In the present study, the OH radical plays a determining role in the photooxidation process of furan, and the NO_x level does not reach the critical value for the NO_x+RO₂ reaction to dominate the process. The main fate of RO₂ is mainly through reaction with HO₂ instead of NO/NO₂, which contributes to SOA formation. Under high RH conditions, the aqueous photochemistry reactions are favored, and contribute to the formation of SOA as we mentioned in Section 3.2, Page 9 in the

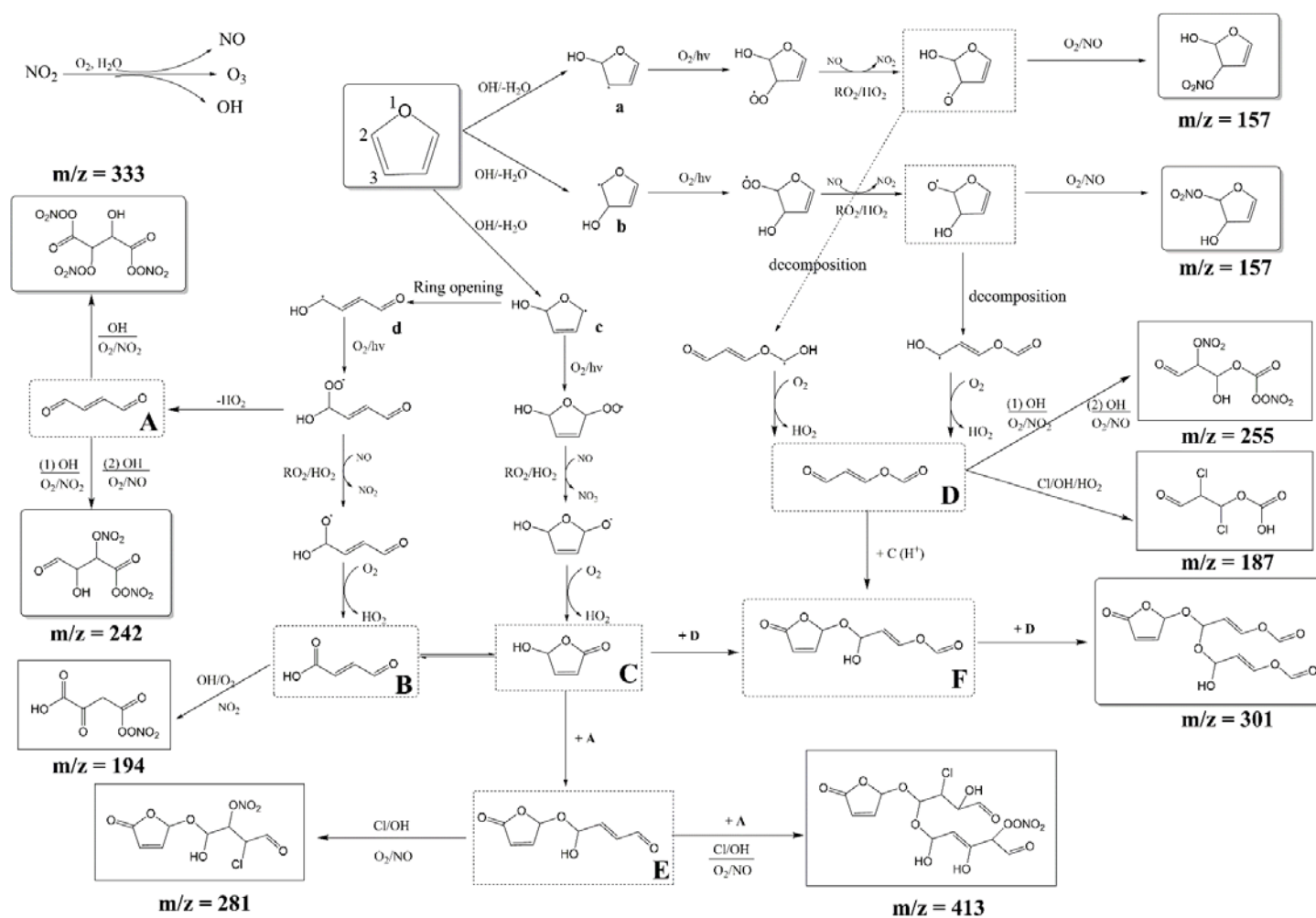
manuscript. Furthermore, the heterogeneous reactions including acid catalyzed reactions at the particle surface promote the formation of first-generation gloxal-like products, which likely play an important role in the process of SOA formation. The proposed mechanism for SOA formation from furan photooxidation is given in a new Section in the revised manuscript as:

“ 3.4 Mechanism of furan SOA formation

According to the identified products in this work and based on previous kinetic (Atkinson et al., 1983; Lee and Tang, 1982) and products (Villanueva et al., 2009; Aschmann et al., 2014a; Tapia et al., 2011; Villanueva et al., 2007; Strollo and Ziemann, 2013) studies reported in the literature, together with tropospheric reactivity principles, a proposed chemical mechanism for SOA formation from furan in the presence of NO_x is shown in Scheme 1. After turning on the lights, NO₂ was converted to NO, accompanied by the formation of the OH radical and O₃. The most efficient oxidant in the present study is the OH radical, for which the rate constant for the reaction with furan is 7 orders of magnitude higher than in the case of O₃ as oxidant (Atkinson et al., 1983). The OH radical is mostly produced by the photolysis of O₃ and HONO (Gligorovski et al., 2015), which are both generated from the cycling of NO_x as presented in Fig. S2 (Stemmler et al., 2006; Li et al., 2008). More extensive studies on gas-phase photochemistry of alkyl furans have shown that the process is initiated by the OH-radical addition to the aromatic ring (Aschmann et al., 2014b; Gomez Alvarez et al., 2009). Additionally, on the basis of well-established mechanisms for atmospheric volatile organic compounds (Atkinson and Arey, 2003), it can be concluded that the reaction is initiated by OH addition to a C=C bond at C2 or C3 positions. Addition at the C2 position forms two cyclic alkyl radicals (a, c), one of which (a) can isomerize to form a ring-opened alkyl radical (d), whereas addition at the C3 position forms a single alkyl radical (b). The OH radical addition leading to a hydrogen abstraction generates the alkyl radicals (R·) followed by reaction with O₂ to form alkylperoxy radicals (RO₂·) (Pan and Wang, 2014). The ring-opened alkylperoxy radical generated from (d) can decompose to generate an unsaturated 1,4-dialdehyde (A). Moreover, the formed alkylperoxy radicals (RO₂·) can either react with RO₂/HO₂ or NO to yield the corresponding alkoxy radical (RO·), which can (i) react with NO/O₂ to form a first-generation peroxydinitrate compound (m/z = 157) (Atkinson, 2000), (ii) react with O₂ to form a first-generation unsaturated products 1,4-aldoacid (B) and hydroxyfuranone (C), or (iii) decompose and then react with O₂ to yield a 1,4-aldoester (D). It is worth mentioning that the hydroxyfuranone (C) can go through a ring-opening reaction via acid-catalyzed heterogeneous/multiphase reactions to form the unsaturated 1,4-aldoacid (B). Scheme 1 also shows the formation of second-generation products (E) and (F) via reactions of the hydroxyfuranone (C) with 1,4-dialdehyde (A) and 1,4-aldoester (D), respectively. As detected by the ESI-Exactive-Orbitrap MS, the hydroxynitrates (m/z = 333, 242) were generated by the reactions of 1,4-dialdehyde (A) with OH radicals and O₂/NO/NO₂ (Carlton et al., 2009; Ervens et al., 2011). There are two pathways for hydroxynitrates formation from RO₂ radicals in the presence of NO_x. According to

which RO₂ radicals may react with NO and NO₂ to form RONO₂ and ROONO₂, respectively (Kroll and Seinfeld, 2008). Hydroxynitrates with m/z = 194 and 255 were produced by similar mechanisms based on 1,4-aldoacid (B) and 1,4-aldoester (D) reactions, respectively. The identified chlorinated organic compounds were generated from the former products (D) and (E), in which hydrogen atoms were substituted by Cl atoms. The OH radicals can convert Cl⁻ ions in the NaCl droplets into Cl atoms, which can rapidly react with organic compounds in the particle-phase and yield identified chlorinated organic compounds (m/z = 281, 413, 187).

As discussed above, the yields of SOA increased with the increase of the NO_x concentration in the present study. Generally, the NO_x level has two different effects in the reaction process. Increasing NO_x concentration will promote the O₃ and HONO formation, leading to more OH radical formed, which in turns is favorable to SOA formation (Sarrafzadeh et al., 2016). In addition, high NO_x level can facilitate the competition between NO/NO₂ and HO₂ to react with RO₂. Products with high volatility will be generated more by the NO_x+RO₂ reaction than by HO₂+RO₂ reaction (Kroll and Seinfeld, 2008). However, the formation of lower volatility products favors the increase of SOA yields (Chen et al., 2018). In this regard, the increasing NO_x level is not conducive to SOA formation. It was shown that the yields of SOA generated from the photooxidation of *m*-xylene increased firstly and then decreased with the increase of the NO_x level (Chen et al., 2018). In the present study, the OH radical plays a determining role in the photooxidation process of furan, and the NO_x level does not reach the critical value for the NO_x+RO₂ reaction to dominate the process. The main fate of RO₂ is mainly through reaction with HO₂ instead of NO/NO₂, which contributes to SOA formation. A previous study on the photooxidation of *m*-xylene/NO_x demonstrated that extremely high NO_x level (*m*-xylene/NO_x < 5.0) suppressed the SOA formation compared to experiments conducted under *m*-xylene/NO_x > 8.0 conditions (Song et al., 2005). Nonetheless, the experimental conditions conducted in the present study did not include the HC:NO_x ratio < 5.0. Consequently, we did not observe a decreasing trend of SOA yield as the NO_x level increased, which is different from the photooxidation of other aromatic compounds where increasing NO_x concentration suppresses the SOA formation. The effect of RH on SOA formation in furan photooxidation is dominantly determined by the aqueous photochemistry under high RH conditions as discussed above. The heterogeneous reactions including acid catalyzed reactions at the surface of particles promote the formation of first-generation gloxal-like products, which likely play an important role in the process of SOA formation. The proposed gloxal-like compound (D) plays a substantial role in the obvious increasing of m/z=187 product formation under high RH conditions. Previously, unsaturated first-generation reaction products of 3-methyl furan have also been suggested to undergo acid-catalyzed condensed-phase reactions, with SOA yields up to 15% (Strollo and Ziemann, 2013). In addition, the reinforced effect of RH on SOA yield was also ascribed from the photooxidations of other aromatic compounds, such as, benzene (Ng et al., 2007), toluene (Hildebrandt et al., 2009; Kamens et al., 2011), and xylene (Zhou et al., 2011).”



Scheme 1: Proposed mechanism for the SOA formation from furan photooxidation. SOA constituents in dotted and solid boxes are proposed first-generation products and ESI-Exactive-Orbitrap MS detected products, respectively.

2. Another weakness of this paper is the lack of context. Based on the introduction and discussion, it seems that furan is being studied because it can be a direct emission or a secondary product. It is not clear if direct emissions of furan are important. The authors seem to group furan together with aromatic compounds such as toluene and m-xylene, but they are quite different (e.g. the SOA yields of furans are an order of magnitude lower than single-ring aromatics). The secondary products from alkane oxidation are dihydrofurans, and are different from furan studied here. The discussion of results does not draw any linkages to these other compounds. So, again, it is not advancing the knowledge of oxidation of alkanes, or aromatic compounds.

Author reply:

Field measurements of hydrocarbon emissions from biomass burning in Brazil has found that furans consists of 52% and 72% of the oxygenated hydrocarbons emissions in the cerrado (grasslands) and selva (tropical forest) regions, respectively (Greenberg et al., 1984). Furan has been proven to be the typical marker species of roasting/burning activities (Gloess et al., 2014; Coggon et al., 2016), which is also an important contribution to OH reactivity towards biomass burning emissions (Gilman et al., 2015). In addition, The reactivity of furans is dominated by 2-methyl furan, 2-furaldehyde, and furan, which have reaction rate coefficients on the order of $\sim 1 \times 10^{-10} \text{ cm}^3 \text{ molecule}^{-1} \text{ s}^{-1}$, roughly equivalent to that of isoprene with major oxidation products including dicarbonyls (Bierbach et al., 1995). Up to 27 furan isomers have been identified from the combustion of Ponderosa Pine. These detected furans constituted a large fraction of the major emitted compounds (similar with benzene, and toluene), indicating that this is an important class of species that should be further explored. (Hatch et al., 2015). Consequently, furan could be an important constituent in the atmosphere. However, SOA formation from these less abundant oxygenated aromatic furans has not been well characterized. Considering the high level of furans detected in previous studies, it is important to assess the SOA formation potential of furans and their role in SOA production in biomass burning plumes. This has been updated in the revised manuscript by inserting the text below on Page 2 while further discussions can be found in our reply to the first comment.

“Originated both from biomass burning and the degradation products of biogenic compounds (Christian et al., 2003; Christian et al., 2004; Greenberg et al., 2006), furan is an important nonmethane volatile organic carbon in the atmosphere. Field measurements of hydrocarbon emissions from biomass burning in Brazil have shown that furans consists of 52% and 72% of the oxygenated hydrocarbons emissions in the cerrado (grasslands) and selva (tropical forest) regions, respectively (Greenberg et al., 1984). Furan has been proven to be the typical marker species of roasting/burning activities (Gloess et al., 2014; Coggon et al., 2016), and is also an important contribution to OH reactivity towards biomass burning emissions (Gilman et al., 2015). In addition, benzene, toluene, and furan have been identified as major compounds emitted from the combustion of Ponderosa Pine, of which up to 27

oxygenated aromatic furans has been observed and constituted a significant fraction (5-37 % by estimated emission factor) of smoke from combustion (Hatch et al., 2015). However, SOA formation from these less abundant oxygenated aromatic furans has not been well characterized. Considering the high level of furans detected in previous studies, it is important to assess the SOA formation potential of furans and their role in SOA production in biomass burning plumes.”

3. I am also concerned about the use of NaCl as a seed. It seems that there may be secondary reactions that the authors are not considering. From the IC results, it seems there is a significant amount of NaNO₃. Assuming the only cations are Na⁺ and H⁺, this would mean some of the chloride from NaCl became HCl, which can volatilize and photolyze in the gas phase to give chlorine atoms, a strong oxidant. In fact, the presence of 1,2-dichloroethane suggests that Cl is reactive and participating in some reactions. Therefore, this photooxidation system is actually quite complicated, with OH, O₃ and Cl reactions all being potential sources of SOA.

Author reply:

In the experiment, NaCl seed acted as the nucleus and facilitated the deposition of semi-volatile organic compounds. Moreover, we totally agree with the Referee that the NaCl seed particles indeed take part in the secondary reactions.

Small particles that act as seed particles for SOA formation are widespread in the atmosphere. NaCl particles used in the present study were used as the seeds in the photooxidation of furan. We conducted an experiment without using NaCl seed particles, and realized no SOA formation under this condition. However, when using NaCl seed particles, the SOA were formed. Furthermore, the formed SOA could easily condense on the surface of NaCl seed particles (Abramson et al., 2013). NaCl seed particles are not only the substrate for vapor-phase condensation, but they also take part in the reactions at the surface. NaCl can react with HNO₃ and N₂O₅, which may influence the O₃ and SOA formation from furan-NO_x irradiations. The NaNO₃ detected by IC is the evidence for secondary reactions taking place. The following sentences were added in the Introduction part, for a better understanding of the aim of adding NaCl seed particles.

Page 2

“Sea salt aerosols are the second most abundant primary inorganic aerosols in the atmosphere, wherein they can play an important role in atmospheric chemistry near coastal regions (Beardsley et al., 2013; Rossi, 2003). They constitute the main components of particulates in the marine troposphere. A previous study has shown that hygroscopic particles act as a sink for volatile organic compounds and take part in the aqueous phase reactions (Volkamer et al., 2007).”

Page 3.

“NaCl particles acted as the nuclei and took part in secondary reactions.”

After turning on the lights, NO₂ was converted into NO, accompanied by the formation of the OH radical and O₃. Although Cl atoms also act as oxidants during the present reaction as could be found from detected products, the most efficient oxidant in the present study is the OH radical, for which the rate constant of the reaction with furan OH is 7 orders of magnitude higher than that in the case of O₃ as oxidant (Atkinson et al., 1983). The oxidation of furan was initiated by the addition of OH radical to form a OH-furan adduct, which reacted with O₂ to produce primary peroxy radicals via O₂ addition. Though the whole reaction process might be complicated, all of the steps were linked via reactions with OH radical, peroxy radicals (RO₂), alkoxy radicals (RO), HO₂, NO, NO₂ and O₂. The detailed mechanism has been explored in the new Section presented in Comment 1 and update in the manuscript on Page 11.

4. Page 4, line 1: the neutralizer is not used to remove charge completely. Rather it is meant to remove excess charge from the atomized solution and bring it closer to charge equilibrium.

Author reply:

We thank the Reviewer for this correction. We have re-written the sentences as:
“An aerosol neutralizer (Model 3087, TSI, USA) was used to bring particles to a steady-state charge equilibrium before they were introduced into the reactor.”

5. Page 5, line 1: NaCl is cubic when dry. Is there correction using the shape factor in obtaining size distribution and volume concentrations?

Author reply:

Indeed, NaCl particles are known to effloresce and form cubic particles. The NaCl seed particles were added as nuclei for the furan photooxidation. During the reactions, the formed products will coat on the cubic NaCl, and change the shape of the particles. As a result, the shape of NaCl detected by SMPS is not cubic in the strict sense. Furthermore, previous studies have shown that solid NaCl particles can carry water as a thin liquid-like surface layer, which also changes the shape of the particles (Allen et al., 1996; Vogt and Finlaysonpitts, 1994). Nevertheless, the shape correction was shown to be not necessary in some similar studies that also used NaCl particles as nuclei for SOA formation (Jia and Xu, 2018; Ge et al., 2017a; Nguyen et al., 2014).

6. Page 5, line 19: what is the potential for organic-bound water being removed from the dryer (leading to overestimation of ALW)?

Author reply:

The drying process for ALW determination we used is based on a widely used method developed by Engelhart (Engelhart et al., 2011). The ALW was calculated as the difference between the particle mass concentrations determined at dry and humid modes, controlled by two Nafion dryers added to the sampling inlet and sheath flow,

respectively. This method has been proven to remove 90% of the water vapor without losing the organic-bound water. Consequently, there is no possibility that the organic-bound water may be removed from the dryer. The following text is inserted on Page 5 to clarify this.

“This DASS method is generally accepted and widely used in the detection of ALW content, and can remove up to 90% of the water vapor without losing the organic-bound water.”

7. Page 5, line 30: there is no prior separation for the ESI-MS. Is there any evidence of matrix effects for quantification?

Author reply:

The ESI-Exactive-Orbitrap MS used in our analysis is not combined to LC and hence, prior separation cannot be conducted. The quantitative analysis of the SOA chemical composition was not made. The data collected from ESI-Exactive-Orbitrap MS were mostly used for the qualitative and semi-quantitative analysis without any influence of matrix effect. The same method has also been used for the analysis of SOA formation from other photooxidation reactions, such as organosulfates formation from the photooxidation of cyclohexene (Liu et al., 2017) and organonitrate formation from irradiations of toluene, isoprene (Jia and Xu, 2018), and propylene (Ge et al., 2017b).

8. Page 5, Page 33: what is the resolution of the mass analyzer?

Author reply:

The mass resolution is 10^5 , and has been updated in the revised manuscript on Page 6.

9. Page 6, line 25 – 26: why is it assumed coagulation is the dominant reason for decrease in number? At a particle concentration of 10^4 cm^{-3} , the homogenous coagulation timescale is on the order of days. Heterogeneous coagulation is likely very fast and would have been completed.

Author reply:

Generally, the decrease in particle number concentration can be summarized by three reasons: coagulation, wall loss, and condensation/evaporation, each of them influencing the number and mass concentration differently. Coagulation changes the number but not mass concentration, wall loss changes number and mass concentration, and condensation changes the mass but not the number concentration (Pierce et al., 2008). Based on this tendency, we concluded that the process affecting the decrease in number concentration is the coagulation. We also tried to find if there is any possibility for the new particle formation to take place, and the contour plots of SOA bursts from the data detected by SMPS were made and are shown in Figure S3. However, we could not find any evidence to support this.

Although there is competition between the formation of new particles and growth of

existing particles by uptake of the precursors, vapor condensation onto existing aerosol particles is favored (Liu et al., 2017). To avoid misunderstanding, we have deleted the sentence “With SOA formation, organics start to dominate and result in the enhanced growth of coagulation, which promote the decay of the particle number concentration”, and added the following sentence on Page 6, 3rd paragraph.

“A previous study conducted in a similar smog chamber showed a decrease in particle number concentration during the experiment (Liu et al., 2017).”

10. Section 3.2: there is extensive discussion of O₃ formation, but this paper is supposed to focus on SOA formation. It is unclear whether such an extensive discussion of O₃ is warranted. It would be great if the authors can tie the O₃ trends to oxidation mechanisms. In fact, the large differences in O₃ may complicate the interpretation, because the relative fractions of OH and O₃ oxidation (rather than NO_x itself) may be driving some of the trends.

Author reply:

The OH radical is mostly produced by the photolysis of O₃ and HONO (Gligorovski et al., 2015), which are both generated from the cycling of NO_x. The O₃ formation was discussed because it is directly linked to the formation of the main oxidant (OH) in the present investigation. After turning on the lights, gas phase NO₂ was converted into NO, accompanied by the formation of the OH radical and O₃. The dominant oxidant in the present study is the OH radical for which the rate constant of the reaction with furan is 7 orders of magnitude higher than in the case of O₃ as oxidant (Atkinson et al., 1983). The oxidation of furan started with the addition of OH radical to form an OH-furan adduct, which reacted with O₂ to produce primary peroxy radicals via O₂ addition. All of the steps involved in the whole process were linked by reactions with OH radical, peroxy radicals (RO₂), alkoxy radicals (RO), HO₂, NO, NO₂ and O₂. A detailed mechanism has been discussed in our reply to Comment 1 and updated in the manuscript.

11. Page 7, line 16: it seems to me that the difference in rate of O₃ increase is within experimental uncertainty. Perhaps error bars should be shown in Figure 3.

Author reply:

Error bars have been added in Figure 3 and Figure 4.

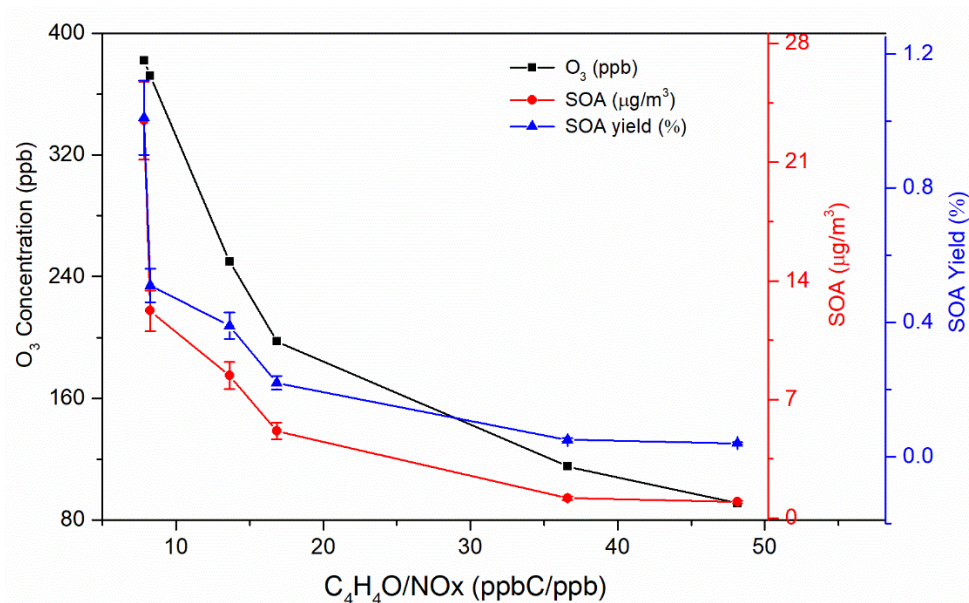


Figure 3: Dependences of the O₃ maximum concentration, SOA mass concentration and SOA yield on the C₄H₄O/NO_x ratio. Since the particle wall loss has a weak RH dependence in our chamber, a mean value of $4.7 \times 10^{-5} \text{ s}^{-1}$ was used for wall loss correction. A density of 1.4 g cm^{-3} was used in SMPS (Jia and Xu, 2018; Kostenidou et al., 2007).

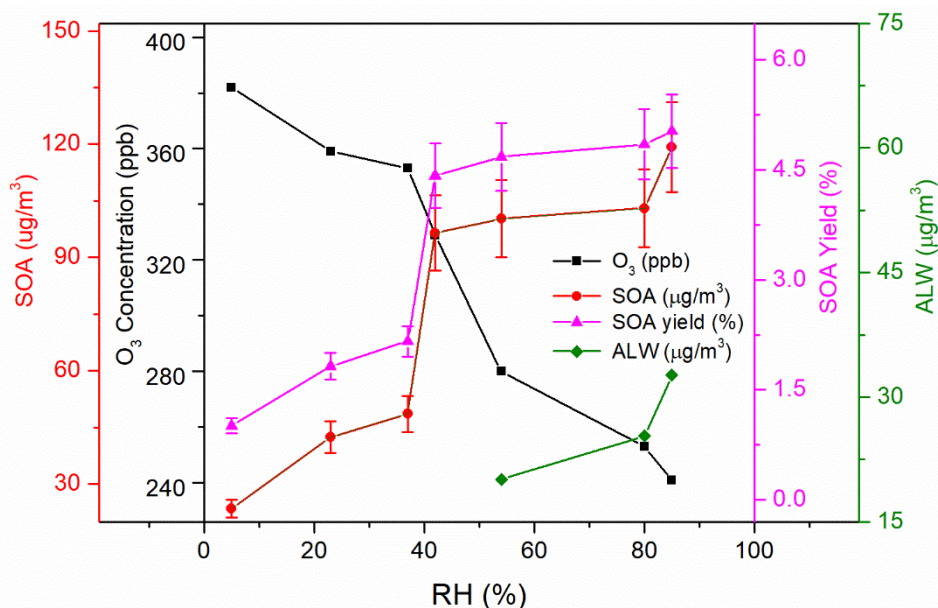


Figure 4: Dependences of O₃ maximum concentration, SOA mass concentration, SOA yield and ALW on relative humidity (RH).

12. Page 9, line 5-6: awkward phrase “equally relevant”?

Author reply:

In the revised manuscript, we have modified the whole sentence as follows:

“However, the particle number distribution under C₄H₄O/NO_x=7.8 and

$C_4H_4O/NO_x=36.6$ conditions show similar profiles”.

13. Section 3.3: all the FTIR results are presented in absolute abundance, i.e. total abundance of each functional group. It is likely more insightful to look at relative abundance, normalized by SOA amount to infer changes in reaction mechanisms. As presented now, it is difficult to see the changes because all functional groups are increasing.

Author reply:

Actually, Figures 6 and 8 in the previous version of the manuscript are presented in relative abundance, which is normalized by the absolute absorbance detected at $C_4H_4O/NO_x=7.8$ and 85 % RH, respectively. To remove any confusion regarding the FTIR results, we have modified the captions of these figures as follows. These figures have now been moved to the Supplement as Figure S4 and Figure S5, respectively.

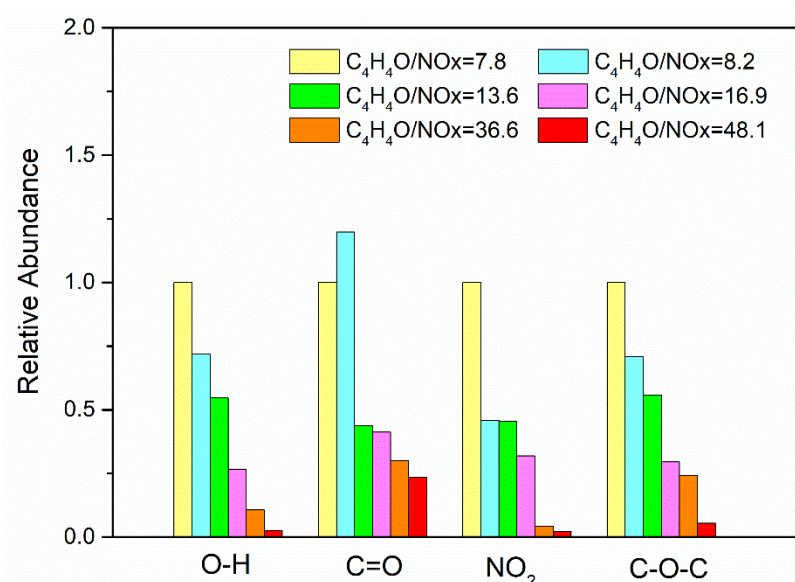


Figure S4: Variations of the relative abundance of different functional groups with C_4H_4O/NO_x ratios from 7.8 to 48.1. Absolute abundances are normalized with respect to the corresponding functional abundance detected at $C_4H_4O/NO_x=7.8$.

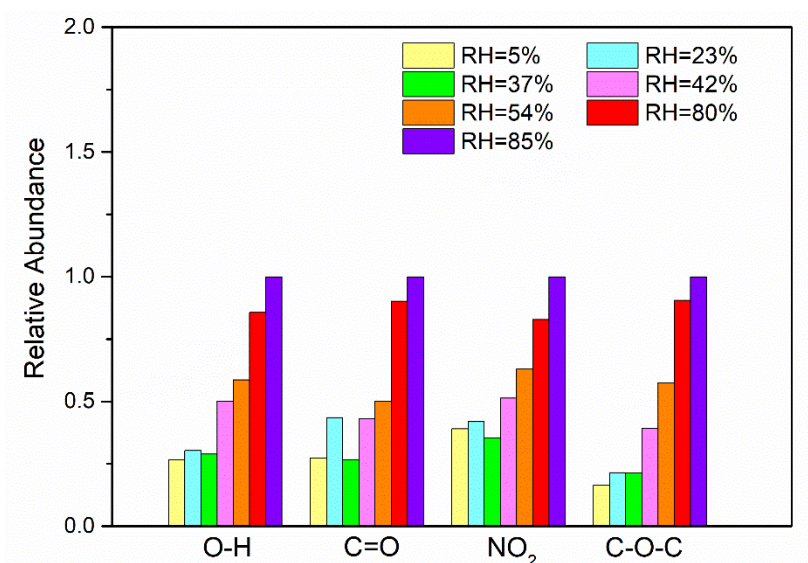


Figure S5: Variations of FTIR absorption abundance of different functional groups at RH from 5 % to 85 % relative to the absolute abundance detected at RH 85 %.

Related sentences on Page 10 have been changed accordingly.

“The calculated variations of the relative abundance of FTIR functional groups at different NO_x levels are presented in Fig. S4, in which the absolute abundances are normalized with respect to the corresponding functional abundance detected at C₄H₄O/NO_x=7.8.”

“The ratio of the absorbance intensities detected at low RH to that at 85 % RH is used as the relative abundance to show more intuitive FTIR results.”

14. Page 10, line 29: I expect N₂O₅ to be quite low under photooxidation conditions.

Author reply:

This assumption is reasonable since N₂O₅ was generated from the gas phase reaction between O₃ and NO₂ (Carter, 2006). A previous study has proven that N₂O₅ is a key product from the VOC-NO_x irradiations (Wang et al., 2016). Our IC results also showed that NaNO₃ can be formed during the experiment. N₂O₅ is probably the main reactant contributing to NaNO₃ formation.

15. Figure 1: Why is 1.4 used as density? Is there literature data that suggest density should be 1.4? Density is likely a function of O/C ratio. Perhaps the authors can justify the use of 1.4 by comparing to literature density data for SOA with similar O/C?

Author reply:

We used this value based on the following reasoning: many studies have estimated that the SOA densities range from 0.9-1.6 g cm⁻³ for a variety of SOA forming systems (Kostenidou et al., 2007; Malloy et al., 2009; Li et al., 2016), and the addition of the NaCl seed particle would also affect the density. Furthermore, the following

densities for selected organic compounds were found: 1.25, 1.48 and 1.42 for trans-cinnamic acid (O/C=1/3), 1,2-acenaphthylenedione (O/C=1/6) and anthraquinone (O/C=1/7), respectively (Kostenidou et al., 2007). Referring to a similar previous study that used NaCl as seed particles (Jia and Xu, 2018), we used 1.4 g cm^{-3} as the density for the furan (O/C=1/4) in the present investigation. The following references were added in the revised manuscript to support our statement on Pages 16 and 18.

Jia, L., and Xu, Y.: Different roles of water in secondary organic aerosol formation from toluene and isoprene, *Atmos. Chem. Phys.*, 18, 8137-8154, 10.5194/acp-18-8137-2018, 2018.

Kostenidou, E., Pathak, R. K., and Pandis, S. N.: An algorithm for the calculation of secondary organic aerosol density combining AMS and SMPS data, *Aerosol Sci. Tech.*, 41, 1002-1010, 10.1080/02786820701666270, 2007.

16. Figure 1, y-axis for number concentration: Is it really just a few particle per cm^3 ? Is there a missing exponent (maybe multiplied by 10^4)?

Author reply:

This was our mistake. There was a 10^4 , which is now updated in the revised figure.

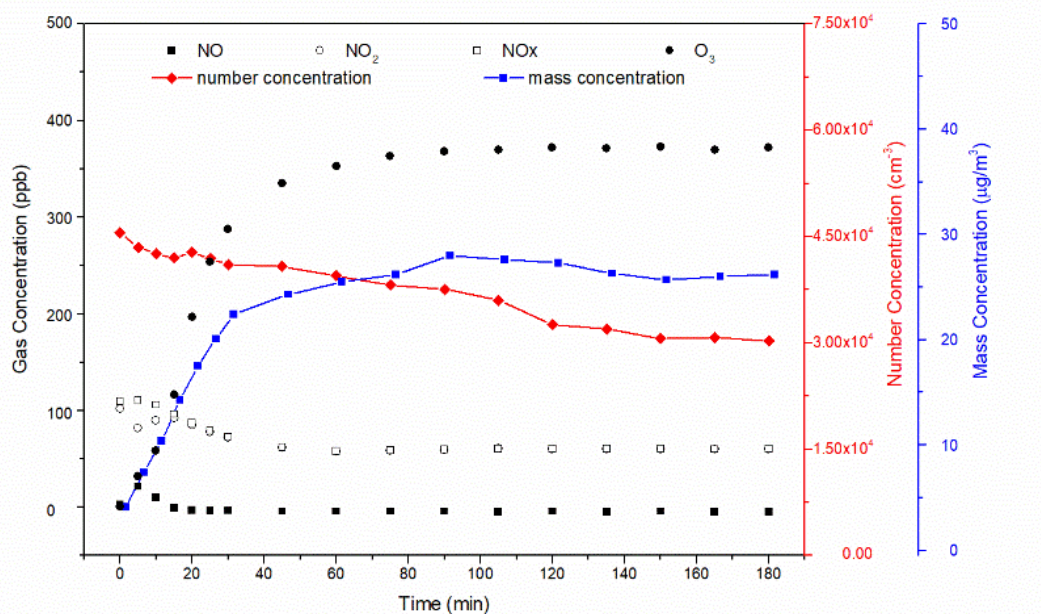


Figure 1: Profile of the gas-phase concentrations of reactants (NO, NO₂, NO_x and O₃) and particle number/mass concentrations (corrected with wall loss) over time. The C₄H₄O/NO_x ratio is 7.9 and RH = 23 %. Since the particle wall loss has a weak RH dependence in our chamber, a mean value of $4.7 \times 10^{-5} \text{ s}^{-1}$ was used for wall loss correction. A density of 1.4 g cm^{-3} was used in the SMPS (Jia and Xu, 2018; Kostenidou et al., 2007).

17. Figure 3: SOA yield should be unitless, or in percent.

Author reply:

The figure has been corrected in the revised manuscript.

18. Table 1: there are too many significant digits, especially in the SOA yields

Author reply:

The number of significant digits in Table 1 has been reduced and updated in the revised manuscript.

Table 1. Summary of initial conditions, O₃ concentrations and particle mass concentrations in furan-NO_x-NaCl photooxidation experiments.

Exp No	Initial conditions						SOA formation results						
	[furan] ₀ (ppb)	[NO] ₀ (ppb)	[NO ₂] ₀ (ppb)	[NO _x] ₀ (ppb)	RH (%)	C ₄ H ₄ O/NO _x (ppbC/ppb)	O ₃ (ppb)	PM ^a (μg m ⁻³)	NaCl ^b (μg m ⁻³)	NaNO ₃ ^c (μg m ⁻³)	ALW ^d (μg m ⁻³)	SOA ^e (μg m ⁻³)	SOA yield (%)
1	708.4	2.2	14.6	16.8	<5 %	48.1	91	12.2	11.3	3.5	--	1.0±0.1	0.04±0.01
2	749.0	2.0	21.2	23.2	<5 %	36.6	115	15.4	10.7	1.6	--	1.2±0.2	0.05±0.01
3	752.5	3.4	41.3	44.7	<5 %	16.9	197	21.3	14.1	2.1	--	5.1±0.5	0.3±0.02
4	705.8	5.5	46.3	51.8	<5 %	13.6	250	23.5	12.6	2.5	--	8.4±0.9	0.3±0.03
5	783.4	6.9	88.0	94.9	<5 %	8.2	372	29.1	13.5	3.9	--	12.2±1.3	0.5±0.05
6	763.4	6.1	91.4	97.5	<5 %	7.8	382	38.6	11.5	3.5	--	23.5±2.3	1.0±0.1
7	764.8	4.1	92.6	96.7	23 %	7.9	359	55.5	10.4	3.8	--	42.3±4.2	1.9±0.2
8	740.1	2.6	94.7	97.3	37 %	7.6	353	64.2	11.2	4.5	--	48.6±4.9	2.2±0.3
9	719.0	5.5	94.7	100.2	42 %	7.2	329	111.1	9.4	5.2	--	96.4±9.7	4.5±0.5
10	704.8	3.3	89.6	92.8	54 %	7.6	280	138.7	12.0	6.2	20.1	100.2±10.1	4.7±0.4
11	699.3	7.4	95.5	102.9	80 %	6.8	253	144.1	8.2	7.6	25.3	103.0±10.3	4.8±0.5
12	780.7	4.7	93.4	98.1	85 %	8.0	241	173.0	10.0	11.1	32.6	119.2±10.4	5.0±0.5
13	750.6	3.9	42.6	46.5	<5 %	16.2	for ESI-Exactive-Orbitrap MS analysis						
14	723.1	5.8	93.4	99.2	<5 %	7.3							
15	740.3	7.4	95.5	102.9	79 %	7.1							

^aPM: particle mass concentration in the chamber was determined from the SMPS and was the sum of NaCl, NaNO₃, ALW, and SOA at the end of the experiments.

5 ^bNaCl: the amount of NaCl at the end of the experiments;

^cNaNO₃: the amount of NaNO₃ at the end of the experiments;

^dALW: the amount of aerosol liquid water content at the end of the experiments;

^eSOA: the amount of secondary organic aerosol at the end of the experiments.

19. Figures 5 and 6 and redundant, same with 7 and 8. In each case, only 1 of the 2 is needed for show changes in functional groups.

Author reply:

As discussed in our reply to comment 13, Figures 5 and 7 show the intuitive FTIR spectra with absolute abundance. Figure 6 and Figure 8 in the manuscript are presented in relative abundance, which is normalized by the absolute absorbance detected at $C_4H_4O/NO_x=7.8$ and 85 % RH, respectively. Following the reviewer's suggestion, Figure 6 and 8 have been moved to the Supplement.

20. Figure 9: It will be useful to highlight the ion peaks described in Table 3. In Table 3, it is difficult to infer trends if the peak abundances are normalized to the highest peak in each spectrum.

Author reply:

Figure 9 has been modified as suggested by the Referee and the new figure is shown below.

We have deleted the normalized results and added the proposed structure of each assigned compound in Table 3.

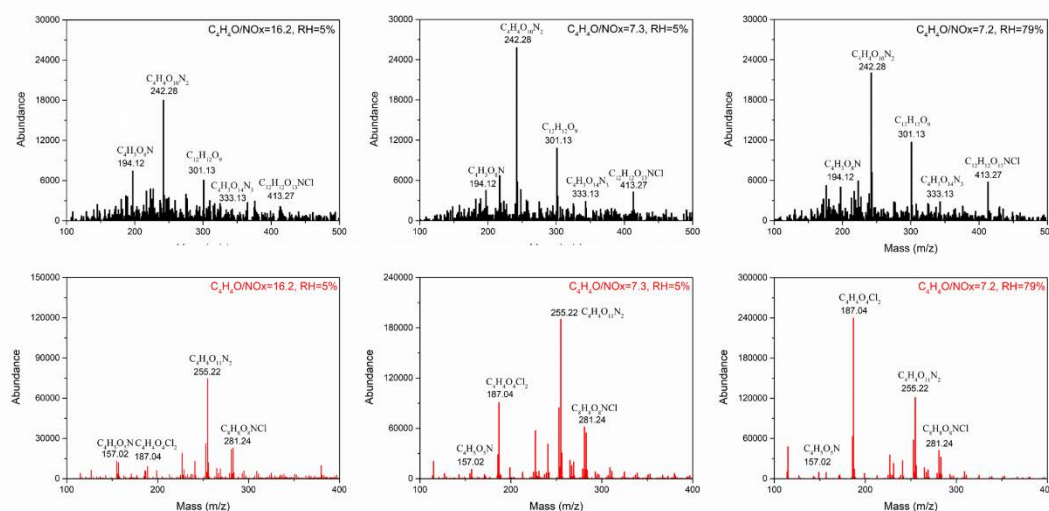


Figure 9: Background-subtracting mass spectra of SOA in both positive ion mode (black) and negative ion mode (red) from the photooxidation of furan under different experimental conditions.

21. Table 2: where would CH₂, CH₃ come from? Furan does not contain any CH₂ or CH₃ groups and I do not expect oxidation to produce any.

Author reply:

Indeed, the absorption frequencies in the range 1515-1350 cm^{-1} are assigned to the bending vibration of the CH group in saturated carbon skeleton. This has been corrected in Table 2.

The sentence on Page 9 has been changed accordingly.

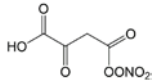
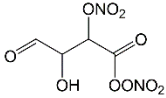
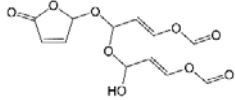
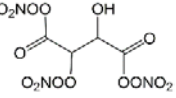
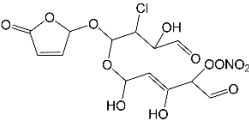
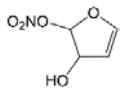
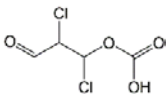
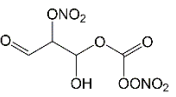
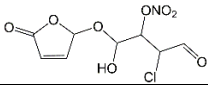
“Correspondingly, the C-H bending vibrations are represented by the absorption between 1350 and 1515 cm^{-1} .”

22. Table 3: Is the mass resolution high enough to calculate exact elemental formula? If so, the exact mass should also be shown to justify elemental formula.

Author reply:

Yes, the exact elemental formula can be calculated based on the exact mass. The exact masses and proposed structures have been added in Table 3.

Table 3. Ion peaks with the assigned compounds observed in the ESI-Exactive-Orbitrap MS. Proposed assignments are based on the formula from ESI-Exactive-Orbitrap MS.

Ion mode	No	Mass (m/z)	Formula	Delta (amu)	RDB	Proposed Structure
	1	194.1181	$\text{C}_4\text{H}_3\text{O}_8\text{N}$	1.131	4	
	2	242.2830	$\text{C}_4\text{H}_4\text{O}_{10}\text{N}_2$	2.298	4	
Positive ion mode	3	301.1378	$\text{C}_{12}\text{H}_{12}\text{O}_9$	1.094	7	
	4	333.1285	$\text{C}_4\text{H}_3\text{O}_{14}\text{N}_3$	0.175	5	
	5	413.2644	$\text{C}_{12}\text{H}_{12}\text{O}_{13}\text{NCl}$	0.267	7	
	6	157.0245	$\text{C}_4\text{H}_5\text{O}_5\text{N}$	-1.995	4	
Negative ion mode	7	187.0410	$\text{C}_4\text{H}_4\text{O}_4\text{Cl}_2$	1.092	2	
	8	255.2295	$\text{C}_4\text{H}_4\text{O}_{11}\text{N}_2$	0.258	4	
	9	281.2476	$\text{C}_8\text{H}_8\text{O}_8\text{NCl}$	0.253	5	

23. It should also be noted that there are far too many grammatical errors in this

manuscript for me to point out. In many cases, these mistakes seriously hinder a reader's ability to understand the science. The manuscript needs to be carefully edited for clarity

Author reply:

We have read through the whole manuscript and corrected the grammatical errors.

References:

- Abramson, E., Imre, D., Beranek, J., Wilson, J., and Zelenyuk, A.: Experimental determination of chemical diffusion within secondary organic aerosol particles, *Phys. Chem. Chem. Phys.*, 15, 2983-2991, 10.1039/c2cp44013j, 2013.
- Allen, H. C., Laux, J. M., Vogt, R., FinlaysonPitts, B. J., and Hemminger, J. C.: Water-induced reorganization of ultrathin nitrate films on NaCl: Implications for the tropospheric chemistry of sea salt particles, *J. Phys. Chem.*, 100, 6371-6375, 10.1021/jp953675a, 1996.
- Aschmann, S. M., Nishino, N., Arey, J., and Atkinson, R.: Products of the OH radical initiated reactions of furan, 2-and 3-methylfuran, and 2,3-and 2,5-dimethylfuran in the presence of NO, *J. Phys. Chem. A*, 118, 457-466, 10.1021/jp410345k, 2014a.
- Aschmann, S. M., Nishino, N., Arey, J., and Atkinson, R.: Products of the OH Radical-Initiated Reactions of Furan, 2-and 3-Methylfuran, and 2,3-and 2,5-Dimethylfuran in the Presence of NO, *J. Phys. Chem. A*, 118, 457-466, 10.1021/jp410345k, 2014b.
- Atkinson, R., Aschmann, S. M., and Carter, W. P.: Kinetics of the reactions of O₃ and OH radicals with furan and thiophene at 298±2 K, *Int. J. Chem. Kinet.*, 15, 51-61, 1983.
- Atkinson, R.: Atmospheric chemistry of VOCs and NO_x, *Atmos. Environ.*, 34, 2063-2101, 10.1016/s1352-2310(99)00460-4, 2000.
- Atkinson, R., and Arey, J.: Atmospheric degradation of volatile organic compounds, *Chem. Rev.*, 103, 4605-4638, 2003.
- Beardsley, R., Jang, M., Ori, B., Im, Y., Delcomyn, C. A., and Witherspoon, N.: Role of sea salt aerosols in the formation of aromatic secondary organic aerosol: Yields and hygroscopic properties, *Environ. Chem.*, 10, 167-177, 10.1071/en13016, 2013.
- Bierbach, A., Barnes, I., and Becker, K.: Product and kinetic study of the OH-initiated gas-phase oxidation of furan, 2-methylfuran and furanaldehydes at ≈ 300 K, *Atmos. Environ.*, 29, 2651-2660, 1995.
- Carlton, A. G., Wiedinmyer, C., and Kroll, J. H.: A review of secondary organic aerosol (SOA) formation from isoprene, *Atmos. Chem. Phys.*, 9, 4987-5005, 10.5194/acp-9-4987-2009, 2009.
- Carter, W. P. L.: The UCR EPA Environmental Chamber, in: *Environmental Simulation Chambers: Application to Atmospheric Chemical Processes*, Dordrecht, 2006, 27-41.
- Chen, Y., Tong, S., Wang, J., Peng, C., Ge, M., Xie, X., and Sun, J.: The effect of Titanium Dioxide on secondary organic aerosol formation, *Environ. Sci. Technol.*, 52, 11612-11620, 10.1021/acs.est.8b02466, 2018.

Christian, T. J., Kleiss, B., Yokelson, R. J., Holzinger, R., Crutzen, P. J., Hao, W. M., Saharjo, B. H., and Ward, D. E.: Comprehensive laboratory measurements of biomass-burning emissions: 1. Emissions from Indonesian, African, and other fuels, *J. Geophys. Res.*, 108, 4719, 10.1029/2003jd003704, 2003.

Christian, T. J., Kleiss, B., Yokelson, R. J., Holzinger, R., Crutzen, P. J., Hao, W. M., Shirai, T., and Blake, D. R.: Comprehensive laboratory measurements of biomass-burning emissions: 2. First intercomparison of open-path FTIR, PTR-MS, and GC-MS/FID/ECD, *J. Geophys. Res.*, 109, D02311, 10.1029/2003jd003874, 2004.

Engelhart, G. J., Hildebrandt, L., Kostenidou, E., Mihalopoulos, N., Donahue, N. M., and Pandis, S. N.: Water content of aged aerosol, *Atmos. Chem. Phys.*, 11, 911-920, 10.5194/acp-11-911-2011, 2011.

Ervens, B., Turpin, B. J., and Weber, R. J.: Secondary organic aerosol formation in cloud droplets and aqueous particles (aqSOA): A review of laboratory, field and model studies, *Atmos. Chem. Phys.*, 11, 11069-11102, 10.5194/acp-11-11069-2011, 2011.

Ge, S., Xu, Y., and Jia, J.: Secondary organic aerosol formation from ethylene ozonolysis in the presence of sodium chloride, *J. Aerosol Sci.*, 106, 120-131, 10.1016/j.jaerosci.2017.01.009, 2017a.

Ge, S., Xu, Y., and Jia, L.: Secondary organic aerosol formation from propylene irradiations in a chamber study, *Atmos. Environ.*, 157, 146-155, 10.1016/j.atmosenv.2017.03.019, 2017b.

Gligorovski, S., Strekowski, R., Barbati, S., and Vione, D.: Environmental Implications of Hydroxyl Radicals (OH), *Chem. Rev.*, 115, 13051-13092, 10.1021/cr500310b, 2015.

Gomez Alvarez, E., Borrás, E., Viidanoja, J., and Hjorth, J.: Unsaturated dicarbonyl products from the OH-initiated photo-oxidation of furan, 2-methylfuran and 3-methylfuran, *Atmos. Environ.*, 43, 1603-1612, 10.1016/j.atmosenv.2008.12.019, 2009.

Greenberg, J. P., Zimmerman, P. R., Heidt, L., and Pollock, W.: Hydrocarbon and carbon-monoxide emissions from biomass burning in Brazil., *J. Geophys. Res.*, 89, 1350-1354, 10.1029/JD089iD01p01350, 1984.

Greenberg, J. P., Friedli, H., Guenther, A. B., Hanson, D., Harley, P., and Karl, T.: Volatile organic emissions from the distillation and pyrolysis of vegetation, *Atmos. Chem. Phys.*, 6, 81-91, 10.5194/acp-6-81-2006, 2006.

Hildebrandt, L., Donahue, N. M., and Pandis, S. N.: High formation of secondary organic aerosol from the photo-oxidation of toluene, *Atmos. Chem. Phys.*, 9, 2973-2986, 2009.

Jia, L., and Xu, Y.: Different roles of water in secondary organic aerosol formation from toluene and isoprene, *Atmos. Chem. Phys.*, 18, 8137-8154, 10.5194/acp-18-8137-2018, 2018.

Kamens, R. M., Zhang, H., Chen, E. H., Zhou, Y., Parikh, H. M., Wilson, R. L., Galloway, K. E., and Rosen, E. P.: Secondary organic aerosol formation from toluene in an atmospheric hydrocarbon mixture: Water and particle seed effects, *Atmos. Environ.*, 45, 2324-2334, 10.1016/j.atmosenv.2010.11.007, 2011.

Kostenidou, E., Pathak, R. K., and Pandis, S. N.: An algorithm for the calculation of secondary organic aerosol density combining AMS and SMPS data, *Aerosol Sci. Tech.*, 41, 1002-1010, 10.1080/02786820701666270, 2007.

Kroll, J. H., and Seinfeld, J. H.: Chemistry of secondary organic aerosol: Formation and evolution of low-volatility organics in the atmosphere, *Atmos. Environ.*, 42, 3593-3624, 10.1016/j.atmosenv.2008.01.003, 2008.

Lee, J. H., and Tang, I. N.: Absolute rate constants for the hydroxyl radical reactions with ethane, furan, and thiophene at room temperature, *J. Chem. Phys.*, 77, 4459-4463, 10.1063/1.444367, 1982.

Li, L., Tang, P., Nakao, S., and Cocker, D. R., III: Impact of molecular structure on secondary organic aerosol formation from aromatic hydrocarbon photooxidation under low-NO_x conditions, *Atmos. Chem. Phys.*, 16, 10793-10808, 10.5194/acp-16-10793-2016, 2016.

Li, S., Matthews, J., and Sinha, A.: Atmospheric hydroxyl radical production from electronically excited NO₂ and H₂O, *Science*, 319, 1657-1660, 10.1126/science.1151443, 2008.

Liu, S., Jia, L., Xu, Y., Tsona, N. T., Ge, S., and Du, L.: Photooxidation of cyclohexene in the presence of SO₂: SOA yield and chemical composition, *Atmos. Chem. Phys.*, 17, 13329-13343, 10.5194/acp-17-13329-2017, 2017.

Malloy, Q. G. J., Nakao, S., Qi, L., Austin, R., Stothers, C., Hagino, H., and Cocker, D. R., III: Real-Time Aerosol Density Determination Utilizing a Modified Scanning Mobility Particle Sizer Aerosol Particle Mass Analyzer System, *Aerosol Sci. Tech.*, 43, 673-678, 10.1080/02786820902832960, 2009.

Ng, N. L., Kroll, J. H., Chan, A. W. H., Chhabra, P. S., Flagan, R. C., and Seinfeld, J. H.: Secondary organic aerosol formation from m-xylene, toluene, and benzene, *Atmos. Chem. Phys.*, 7, 3909-3922, 10.5194/acp-7-3909-2007, 2007.

Nguyen, T. B., Coggon, M. M., Bates, K. H., Zhang, X., Schwantes, R. H., Schilling, K. A., Loza, C. L., Flagan, R. C., Wennberg, P. O., and Seinfeld, J. H.: Organic aerosol formation from the reactive uptake of isoprene epoxydiols (IEPOX) onto non-acidified inorganic seeds, *Atmos. Chem. Phys.*, 14, 3497-3510, 10.5194/acp-14-3497-2014, 2014.

Pan, S., and Wang, L.: Atmospheric Oxidation Mechanism of m-Xylene Initiated by OH Radical, *J. Phys. Chem. A*, 118, 10778-10787, 10.1021/jp506815v, 2014.

Pierce, J. R., Engelhart, G. J., Hildebrandt, L., Weitkamp, E. A., Pathak, R. K., Donahue, N. M., Robinson, A. L., Adams, P. J., and Pandis, S. N.: Constraining particle evolution from wall losses, coagulation, and condensation-evaporation in smog-chamber experiments: Optimal estimation based on size distribution measurements, *Aerosol Sci. Tech.*, 42, 1001-1015, 10.1080/02786820802389251, 2008.

Rossi, M. J.: Heterogeneous reactions on salts, *Chem. Rev.*, 103, 4823-4882, 10.1021/cr020507n, 2003.

Sarrafzadeh, M., Wildt, J., Pullinen, I., Springer, M., Kleist, E., Tillmann, R., Schmitt, S. H., Wu, C., Mentel, T. F., and Zhao, D.: Impact of NO_x and OH on secondary organic

aerosol formation from β -pinene photooxidation, *Atmos. Chem. Phys.*, 16, 11237-11248, 2016.

Song, C., Na, K. S., and Cocker, D. R.: Impact of the hydrocarbon to NO_x ratio on secondary organic aerosol formation, *Environ. Sci. Technol.*, 39, 3143-3149, 10.1021/es0493244, 2005.

Stemmler, K., Ammann, M., Donders, C., Kleffmann, J., and George, C.: Photosensitized reduction of nitrogen dioxide on humic acid as a source of nitrous acid, *Nature*, 440, 195-198, 10.1038/nature04603, 2006.

Strollo, C. M., and Ziemann, P. J.: Products and mechanism of secondary organic aerosol formation from the reaction of 3-methylfuran with OH radicals in the presence of NO_x, *Atmos. Environ.*, 77, 534-543, 10.1016/j.atmosenv.2013.05.033, 2013.

Tapia, A., Villanueva, F., Salgado, M. S., Cabanas, B., Martinez, E., and Martin, P.: Atmospheric degradation of 3-methylfuran: kinetic and products study, *Atmos. Chem. Phys.*, 11, 3227-3241, 10.5194/acp-11-3227-2011, 2011.

Villanueva, F., Barnes, I., Monedero, E., Salgado, S., Gómez, M. V., and Martin, P.: Primary product distribution from the Cl-atom initiated atmospheric degradation of furan: Environmental implications, *Atmos. Environ.*, 41, 8796-8810, 10.1016/j.atmosenv.2007.07.053, 2007.

Villanueva, F., Cabañas, B., Monedero, E., Salgado, S., Bejan, I., and Martin, P.: Atmospheric degradation of alkylfurans with chlorine atoms: Product and mechanistic study, *Atmos. Environ.*, 43, 2804-2813, 10.1016/j.atmosenv.2009.02.030, 2009.

Vogt, R., and Finlaysonpitts, B. J.: A diffuse-reflectance infrared fourier-transform spectroscopic (DRIFTS) study of the surface-reaction of NaCl with gaseous NO₂ and HNO₃, *J. Phys. Chem.*, 98, 3747-3755, 10.1021/j100065a033, 1994.

Volkamer, R., Martini, F. S., Molina, L. T., Salcedo, D., Jimenez, J. L., and Molina, M. J.: A missing sink for gas-phase glyoxal in Mexico City: Formation of secondary organic aerosol, *Geophys. Res. Lett.*, 34, L19807, 10.1029/2007gl030752, 2007.

Wang, Y., Luo, H., Jia, L., and Ge, S.: Effect of particle water on ozone and secondary organic aerosol formation from benzene-NO₂-NaCl irradiations, *Atmos. Environ.*, 140, 386-394, 10.1016/j.atmosenv.2016.06.022, 2016.

Zhou, Y., Zhang, H., Parikh, H. M., Chen, E. H., Rattanavaraha, W., Rosen, E. P., Wang, W., and Kamens, R. M.: Secondary organic aerosol formation from xylenes and mixtures of toluene and xylenes in an atmospheric urban hydrocarbon mixture: Water and particle seed effects (II), *Atmos. Environ.*, 45, 3882-3890, 10.1016/j.atmosenv.2010.12.048, 2011.